



HAL
open science

Stemness markers characterize IGR-CaP1, a new cell line derived from primary epithelial prostate cancer

Anne Chauchereau, Nader Al Nakouzi, Catherine Gaudin, Sylvestre Le Moulec, Daniel Compagno, Nathalie Auger, Jean Bénard, Paule Opolon, François Rozet, Pierre Validire, et al.

► **To cite this version:**

Anne Chauchereau, Nader Al Nakouzi, Catherine Gaudin, Sylvestre Le Moulec, Daniel Compagno, et al.. Stemness markers characterize IGR-CaP1, a new cell line derived from primary epithelial prostate cancer. *Experimental Cell Research*, 2011, 317 (3), pp.262-275. 10.1016/j.yexcr.2010.10.012 . hal-03211032

HAL Id: hal-03211032

<https://hal.science/hal-03211032>

Submitted on 28 Apr 2021

HAL is a multi-disciplinary open access archive for the deposit and dissemination of scientific research documents, whether they are published or not. The documents may come from teaching and research institutions in France or abroad, or from public or private research centers.

L'archive ouverte pluridisciplinaire **HAL**, est destinée au dépôt et à la diffusion de documents scientifiques de niveau recherche, publiés ou non, émanant des établissements d'enseignement et de recherche français ou étrangers, des laboratoires publics ou privés.

available at www.sciencedirect.comwww.elsevier.com/locate/yexcr

Research Article

Stemness markers characterize IGR-CaP1, a new cell line derived from primary epithelial prostate cancer

Anne Chauchereau^{a,h,*}, Nader Al Nakouzi^{a,h}, Catherine Gaudin^{a,h}, Sylvestre Le Moulec^{a,h}, Daniel Compagno^b, Nathalie Auger^{c,h}, Jean Bénard^{c,h}, Paule Opolon^{d,h}, François Rozet^e, Pierre Validire^f, Gaëlle Fromont^g, Karim Fizazi^{a,h}

^aProstate Cancer Group, INSERM U981, Institut Gustave Roussy, Villejuif, F-94805, France

^bLaboratory of Prostate Cancer, Dep. Química Biológica-University of Buenos-Aires-FCEyN, Buenos-Aires, Argentina

^cDepartment of Medical Biology and Pathology, Institut Gustave Roussy, Villejuif, F-94805, France

^dUMR8121, Institut Gustave Roussy, Villejuif, F-94805, France

^eDepartment of Urology, Institut Mutualiste Montsouris, Paris, F-75014, France

^fDepartment of Pathology, Institut Mutualiste Montsouris, Paris, F-75014, France

^gDepartment of Pathology, CHU-University of Poitiers, Poitiers, F-86000, France

^hUniversity Paris-Sud 11, France

ARTICLE INFORMATION

Article Chronology:

Received 12 April 2010

Revised version received

20 September 2010

Accepted 16 October 2010

Keywords:

Prostatic neoplasms

Tumor cells cultured

Basal epithelial cells

Tumor stem cells

Gene expression profiling

ABSTRACT

Deciphering molecular pathways involved in the early steps of prostate oncogenesis requires both *in vitro* and *in vivo* models derived from human primary tumors. However the few recognized models of human prostate epithelial cancer originate from metastases. To date, very few models are proposed from primary tumors and immortalizing normal human prostate cells does not recapitulate the natural history of the disease. By culturing human prostate primary tumor cells onto human epithelial extra-cellular matrix, we successfully selected a new prostate cancer cell line, IGR-CaP1, and clonally-derived subclones. IGR-CaP1 cells, that harbor a tetraploid karyotype, high telomerase activity and mutated TP53, rapidly induced subcutaneous xenografts in nude mice. Furthermore, IGR-CaP1 cell lines, all exhibiting negativity for the androgen receptor and PSA, express the specific prostate markers alpha-methylacyl-CoA racemase and a low level of the prostate-specific membrane antigen PSMA, along with the prostate basal epithelial markers CK5 and CK14. More importantly, these clones express high CD44, CD133, and CXCR4 levels associated with high expression of $\alpha 2\beta 1$ -integrin and Oct4 which are reported to be prostate cancer stemness markers. RT-PCR data also revealed high activation of the Sonic Hedgehog signalling pathway in these cells. Additionally, the IGR-CaP1 cells possess a 3D sphere-forming ability and a renewal capacity by maintaining their CSC potential after xenografting in mice. As a result, the hormone-independent IGR-CaP1 cellular clones exhibit the original features of both basal prostate

* Corresponding author. Prostate Cancer Group, INSERM U981, Institut Gustave Roussy, 114 rue Edouard Vaillant, Villejuif, F-94805, France. Fax: + 33 1 42 11 60 94.

E-mail addresses: anne.chauchereau@igr.fr (A. Chauchereau), nader.nakouzi@igr.fr (N. Al Nakouzi), catherine.gaudin@igr.fr (C. Gaudin), sylvestre.lemoulec@gmail.com (S. Le Moulec), danielcompagno@qb.fcen.uba.ar (D. Compagno), nathalie.auger@igr.fr (N. Auger), jean.benard@igr.fr (J. Bénard), paule.opolon@igr.fr (P. Opolon), francois.rozet@imm.fr (F. Rozet), pierre.validire@imm.fr (P. Validire), g.fromont@chu-poitiers.fr (G. Fromont), karim.fizazi@igr.fr (K. Fizazi).

0014-4827/\$ – see front matter © 2010 Published by Elsevier Inc.

doi:10.1016/j.yexcr.2010.10.012

tissue and cancer stemness. Tumorigenic IGR-CaP1 clones constitute invaluable human models for studying prostate cancer progression and drug assessment *in vitro* as well as in animals specifically for developing new therapeutic approaches targeting prostate cancer stem cells.

© 2010 Published by Elsevier Inc.

Introduction

Prostate cancer is the second leading cause of cancer-related deaths in men in North America and Europe. Nowadays, there is still no cure available for patients with advanced disease especially when hormone independence emerges [1]. Cell cultures established directly from primary tumors from patients are powerful research resources for studying cancer cell biology and for developing new strategies against cancer. However, human prostate cells are known to be one of the most difficult tissues to develop in a continuously growing culture especially while maintaining hormone dependency. Most *in vitro* or xenografted models of prostate cancer have been established from metastases [2,3]. The immortalization of normal human prostate cells, either epithelial or stromal, has been proposed to extensively investigate the early genetic events that give rise to epithelial prostate cancer progression. However, to date, these artificial models have been unable to identify the cells that initiate prostate cancer. Clearly, due to difficulties inherent to *in vitro* culture, models directly derived from primary tumors are still lacking. In spite of huge efforts, only two continuously cultured human primary epithelial prostate cancer cell lines have been established, the E006AA [4] and the HH870 [5] cell lines but they have not been documented so far, except for a recent study of AR signalling in the E006AA cell line [6]. A third human prostate cancer model was recently established *in vitro* from a trans-rectal prostate needle biopsy specimen but it was unable to grow in nude mice [7]. Currently, prostate cancer models, directly derived from primary tumors, enabling both *in vivo* and *in vitro* approaches and representing the early stages of this cancer are still lacking.

Regarding homeostasis of prostate tumor cells, there is mounting evidence that prostate cancer results from a hierarchical model originating from rare cancer stem cells (CSC) that enables tumor maintenance [8]. Based on this model, it has been suggested that androgen-independent stem cells give rise to two types of cells, stem cells and androgen-independent transit-amplifying cells, capable of differentiating into luminal cells. Prostate cancer stem/progenitor cells may exhibit similar characteristics to those of normal stem cells likely localized in the basal cell compartment [9]. Collins et al. [10] first identified and isolated prostate stem cells from primary tumors. It was subsequently shown that these cells express CD44, $\alpha 2\beta 1$ -integrin and CD133, normal prostate epithelial stem cell markers [11,12]. Recently, telomerase-immortalized basal prostate epithelial cell (HPET) lines were obtained which provide a constant supply of cells while simultaneously maintaining the differentiation characteristics of the original tissue [13]. Clonally-derived HPET cells reconstitute the original human tumor *in vivo* and differentiate into the three prostate epithelial cell lineages, indicating a common stem/progenitor cell [14]. More recently, prostatic epithelial RC-165N/hTERT cells were obtained which exhibit a stable stem cell phenotype CD133⁺/CD44⁺/ $\alpha 2\beta 1$ ⁺/34 β E12⁺/CK18⁺/p63⁻/AR⁻/PSA⁻ and the ability to differentiate into AR-positive cell types *in vitro* [15,16]. Most of these

cancer stem cells were identified using surface markers that recognize their corresponding normal tissue stem and progenitor cells, thus strengthening the resemblance between tumor development and normal prostate organogenesis. Until now, these markers essentially pinpoint cell populations with CSC characteristics.

Here, we describe the establishment and characterization of a new prostate cancer cell line and cell-derived clones from a primary tumor. These cells show phenotypic features of prostate epithelial basal cells, exhibit the original features of prostate tissue and retain cancer stem cell properties. Thus, our new IGR-CaP1 models may help develop new therapeutic approaches that target prostate cancer stem cells.

Materials and methods

Primocultures and cell cultures

After mechanical dissociation of human prostate tumor tissue and counting, cells were seeded on an extracellular matrix (ECM) of human epithelial origin, IGR-XC, and further cultured in RPMI medium supplemented with 10% FBS (foetal bovine serum, Gibco), penicillin-streptomycin antibiotics and fungizone. This human ECM, developed at the *Institut Gustave Roussy*, Villejuif, France (IGR-XC, US patent 7,476,496), prevents anoikis and enables epithelial cells to anchor onto the substrate [17]. Primoculture conditions combined IGR-XC ECM and proline-depleted RPMI medium to prevent fibroblast contamination [18]. The cells were incubated at 37 °C with 5% CO₂ until they reached semi-confluence and were then trypsinized. After maintaining these culture conditions for 20 passages, cells were allowed to grow onto plastic flasks in regular RPMI medium containing 10% FBS and antibiotics. The renowned prostate cancer cell lines LNCaP and PC3 were cultured in RPMI-1640 containing 10% FBS and MDA-PCa-2b cells, as previously described [19]. To re-establish *in vitro* cultures after xenografting into nude mice, xenografted tumors ($n = 5$) were collected when they attained 300 mm³. Tumor cells were dissociated by a 30 min digestion at 37 °C with Collagenase H/DNase I (Roche) in culture medium, as previously described [20] and plated in 6-well cell culture dishes in classic culture medium. Forty-eight hours after, the medium was replaced by proline-depleted RPMI medium and cells were cultured for 5 passages.

Clinical summary

The prostate primary tumour samples were collected from the Institut Mutualiste Montsouris (Paris, France) from 3 patients in accordance with protocols approved by the local ethics committees. The prostate cancer tissue that yielded the IGR-CaP1 cell line was obtained from a 58-year-old Caucasian French patient who had undergone a radical prostatectomy for clinically localized prostate cancer. At diagnosis, the serum PSA level was 5.6 ng/ml.

- 157 Pathological analysis of the prostatectomy specimen revealed a
158 massive bilateral posterior tumor confined to the prostatic capsule
159 which was a moderately-differentiated adenocarcinoma with a
160 Gleason score of 7 [4(70%) + 3(30%)]. The clinical stage assigned
161 was pT2c Nx.
- 162 **Cell growth kinetics**
- 163 Cell growth kinetics was determined by counting the number of
164 viable cells at regular intervals. After seeding in triplicate at 4000
165 cells/well in 12-well plates in normal culture medium or in
166 medium containing 10% charcoal-stripped FBS, cells were trypsi-
167 nized daily, stained with trypan blue and counted. The doubling
168 time was calculated from the regression equation of the curve. For
169 the hormone-dependent growth assay, cells were seeded at 10 000
170 cells/well in 96-well plates. After 24 h, the culture medium was
171 replaced with phenol red-free medium containing 10% charcoal-
172 stripped FBS and dihydrotestosterone (DHT) was added or not, at a
173 final concentration of 10^{-9} M. The medium was replaced each day.
174 After 72 h, cell survival was measured with the WST1 test (Roche).
- 175 **Telomerase assay**
- 176 Telomerase activity was measured by using the Biomax Telomerase
177 detection kit (Biomax Inc., MD, US) based on a quantitative
178 real-time telomeric repeat amplification protocol, according to the
179 manufacturer's recommendations. Telomerase activity was deter-
180 mined through its ability to synthesize telomeric repeats onto an
181 oligonucleotide substrate in cellular extracts and the resulting
182 extended products were amplified by PCR (35–40 cycles) using the
183 DNA SYBR Green fluorochrome and measured on a 7900HT Fast
184 Real-Time PCR System (Applied Biosystems). Telomerase activity
185 was quantified according to the manufacturer's recommendations
186 against a standard curve that had an R^2 of 0.98.
- 187 **DNA sequencing for analysis of TP53 mutation**
- 188 Sequencing was performed from cDNA as previously described
189 [21]. Two different DNA preparations obtained from different cell
190 aliquots showed the same Tp53 mutation.
- 191 **Karyotype**
- 192 Metaphases were harvested after a 2.5-h colchicine block. Chromo-
193 some spreads were obtained according to previously described
194 techniques [22]. Karyotypes were established on more than 10
195 metaphases after R-banding according to the standardized human
196 karyotype.
- 197 **Short tandem repeat DNA typing (STR typing)**
- 198 Genomic DNA extracted from the cells was prepared using the
199 QIAamp DNA Micro kit (Qiagen) and was quantified using real-
200 time PCR technology. The short tandem repeat (STR) analysis was
201 conducted using the multiplex-PCR-based Identifiler amplifica-
202 tion kit (Applied Biosystems) on 1 ng of genomic DNA in which 16
203 STR loci were simultaneously co-amplified. Automated DNA
204 fragment analysis was performed on an ABI3130xl Genetic
205 Analyser. Fluorescent data were collected and analyzed using
206 GeneMapper 3.2 ID-specific genotyping software (Applied Bio-
systems). The resulting profile showed the assigned allele values
corresponding to the number of repeat units identified for each
locus.
- 207
208
209
- 210 **In vivo tumorigenicity assay**
- 211 Six-week-old male athymic nude mice (NC-nu/nu) (Janvier,
212 France) were used in conformity with the Guidelines of the French
213 Government regarding operative procedures and animal care. IGR-
214 CaP1 cells (10^7) were subcutaneously injected into the dorsal side
215 without matrigel. Orthotopic injections were performed, as
216 previously described [23]. Briefly, the prostate of each anesthe-
217 tized mouse was exposed via a midline laparotomy incision and
218 10^6 cells in 5 μ l PBS were directly injected into the prostate.
- 219 **Western blot analysis**
- 220 Western Blot assays were performed on 50 μ g of whole cellular
221 lysates. Blots were probed with anti-AR (N-20) or anti-PSA
222 antibody (C-19) from SantaCruz, or anti-Oct4 antibody (Chemi-
223 con). Immunoblot analyses were developed using the enhanced
224 chemoluminescence-based detection kit (Pierce).
- 225 **Flow cytometry**
- 226 FACS analysis was used to determine differentiation marker
227 expression and to sort cells. For cytoplasmic or nuclear proteins,
228 permeabilization in 0.25% triton X-100 was performed before
229 labelling. The following antibodies were used: anti-human
230 EpCAM-PE (clone EBA-1, Becton Dickinson), PSMA-FITC (clone
231 107-1A4, MBL medical), CK5/8-FITC (clone 5F173, US-Biological),
232 CK8-FITC (clone B22.1, GeneTex), CK14-FITC (clone 2Q1030, US-
233 Biological), CK18-FITC (abcam), CD24-FITC (clone ML-5, BD
234 pharmingen), CD44-FITC (clone G44-26, BD Biosciences), CD133-
235 APC (AC133, Miltenyi-Biotec), CXCR4-PE (also named CD184-PE,
236 clone 12G5, BD Biosciences), P504S (AMACR) (2A10F3, Santa
237 Cruz). The corresponding isotype control antibodies were included
238 in each staining condition. For indirect labelling, purified mouse
239 IgG2b and rabbit IgG (R&D System) were used as isotype controls
240 and Molecular Probes' Alexa Fluor 488 (1:200) were used as
241 secondary antibodies. Samples were analyzed with the FACS
242 Calibur cytometer (Becton Dickinson).
- 243 **TaqMan real-time quantitative reverse transcription-PCR
analysis**
- 244 Total RNA was extracted from cell lines using the RNeasy Midi kit
245 (Qiagen) and 1 μ g of RNA was reversed transcribed using random
246 hexamers (Applied Biosystems). Quantitative real-time PCR was
247 performed with the ABI Prism 7900 Sequence Detection System
248 (Applied Biosystems) using 5 μ l of 1:20 diluted cDNA in a final
249 volume of 25 μ l according to the manufacturer's recommenda-
250 tions. The reference and sequence of PCR primers and probes were
251 designed by Applied Biosystems (see Supplementary Material)
252 and used according to the manufacturer's recommendations. The
253 amount of sample RNA was normalized by amplification of an
254 endogenous control (18S). In each experiment, the relative
255 quantification of the transcripts was derived using the standard
256 curve method. Results obtained in the IGR-CaP1 cells were
257 compared to that found in LNCaP cells.
- 258
259

259 Immunohistochemistry (IHC)

260 The different tissue specimens (primary tumors and potentially
261 metastatic organs) from mice were fixed in Finefix (Milestone
262 Medical), and then paraffin sections (4 μ thick) were processed
263 and stained with hematoxylin–eosin–safranin (HES). Tumor and
264 organ sections were incubated with anti-pan-CK (AE1/AE3/PCK26
265 (APK), Ventana Medical Systems), anti-p53 (Ventana Medical
266 Systems), anti-PSMA (3E6) or anti-PAP (PASE/4LJ) from Diagnostic
267 BioSystems, anti-Ki67 (Zymed), anti-CK14 (LL001, R&D Systems)
268 antibodies. All sections were analyzed using a Zeiss Axiophot
269 microscope and a SensiCam PCO digital camera. Representative
270 views were taken at 100 \times magnification.

271 Immunofluorescence microscopy

272 Cells were fixed in 4% formaldehyde, washed and then incubated
273 with goat serum solution (1:100) and anti-human α 2 β 1-integrin
274 antibody (BHA2.1, Chemicon) followed by incubation with Alexa-
275 Fluor 488 antibody (Molecular Probes). Nuclei were stained with
276 Dapi vectashield mounting reagent (Vector Laboratories). Images
277 were acquired on a Zeiss Axioplan 2 microscope.

278 Spheroid soft agar assay

279 Prostate spheroid cultures were made from IGR-CaP1 cells (P30). Cells
280 were seeded at 10 000 cells/well in 12-well plates in 0.35% agarose in
281 growth medium overlaid on a base of 0.8% agarose. Cultures were fed
282 every 4–5 days for 2 weeks until colonies were formed. The 3D
283 cultures were performed in classic RPMI medium supplemented with
284 FBS. Cells grown as nonadherent spherical clusters were fixed in
285 Finefix (Milestone Medical), collected using the cytoblock kit (Thermo
286 laboratories) and embedded in paraffin. Then paraffin sections (4 μ
287 thick) were processed and stained with HES.

288 Results

290 The IGR-CaP1 cell line is a prostate cancer epithelial cell line

291 In a combination of ECM of human epithelial origin, IGR-XC and
292 medium—which avoids fibroblast overgrowth—primary tumor frag-
293 ments from three patients with localized disease were seeded and only
294 one tumor fragment, from a 58-year-old prostate cancer patient,
295 generated stabilized tumor cells after 20 subcultures *in vitro*. These
296 cells were spontaneously immortalized since they were able to grow
297 on plastic dishes in classic culture medium while retaining their
298 proliferative capacity in a continuous long-term culture (up to 50
299 passages). They grew as adherent cells with epithelial cell morphology
300 (Fig. 1A) and expressed the epithelial cell adhesion molecule EpCAM
301 (Fig. 1B) as compared with the isotypic control or EpCAM-negative
302 human fibroblasts IMR90 (not shown). They also stained positively for
303 cytokeratin, as observed in the original tumor (Fig. 1C–D), confirming
304 the epithelial origin of this cell line. The absence of chromogranin A
305 expression in IGR-CaP1 cells led us to rule out the hypothesis of
306 neuroendocrine cells while the lack of the mesenchymal markers
307 STRO-1, CD73 and CD105 (not shown) and proline-depleted medium
308 used to establish the cell line rather suggested that these cells did not
309 correspond to mesenchymal cells either.

IGR-CaP1 cell identification by genomic profiling analyses 310

To better characterize the cell line, genotyping of the complete
311 Short Tandem Repeat (STR) profile was performed on total DNA
312 from the IGR-CaP1 cell line (Table 1). This technique allowed
313 definitive cell line authentication. The profiles confirmed the
314 complexity of the karyotype (Fig. 2A) and showed the absence of
315 the Y chromosome on the amelogenin locus. We observed the
316 same STR profile between DNA prepared from IGR-CaP1 cells at
317 passages 10 and 50, showing that chromosome alterations were
318 conserved throughout cultures. Since establishing a primary cell
319 culture may generate cellular heterogeneity, we undertook clonal
320 selection from the parental IGR-CaP1 cells by limit dilutions and
321 obtained nine clonally-derived clones. To definitively identify two
322 of them, named 3A11 and 3C11, the STR profile was determined
323 and showed some minor differences compared with that of the
324 parental IGR-CaP1 cell line (Table 1). Allelic changes were
325 observed at two loci vWA and D18S51, for the 3A11 derived
326 clone and at 5 loci D2S1338, D19S433, D18S51, D5S818 and FGA
327 for the 3C11 derived clone. 328

Karyotypic analysis was performed on the IGR-CaP1 cell line at
329 passage 29 using a conventional R-banding technique. The analysis
330 showed a complex tetraploid karyotype with 86–91 chromosomes,
331 including numerical and structural rearrangements (Fig. 2A). The
332 karyotype was determined to be 86–89 <4n>,XX,+der(X),+der
333 (X),-Y,-Y, der(1)t(1;?)(p32;?), add(2)(q3?2), -3,der(3)t(3;?)
334 (p10;?), -4, -4, -5, -5, -6, -6,ins(7;?)(p15;?),+8,+8,+11,
335 +11, -13, -13, add(13)(q31), -14, -15, -15,del(18)(q22),del
336 (18(q22),+20,del(20)(q12),+del(20)(q12),+mar inc[cp15]. 337

IGR-CaP1 cells spontaneously express high telomerase activity and show malignant features *in vitro* 338

Telomerase, the enzyme responsible for replicating telomeres, is
340 expressed at a low level in most normal tissues and becomes
341 activated during tumorigenesis. As telomerase expression can
342 itself induce immortalization [24], we measured the telomerase
343 activity in IGR-CaP1 cell extracts using a quantitative PCR system
344 targeting telomere extension products. The spontaneously im-
345 mortalized IGR-CaP1 cells exhibited high telomerase activity
346 compared with normal lymphocytes (PBL) (Fig. 2B). However,
347 this activity was lower than that measured in the PC3 cells derived
348 from a metastatic site. 349

Since mutations in the tumor suppressor gene *Tp53* are
350 frequently associated with chromosome instability, *Tp53* expres-
351 sion was examined in IGR-CaP1 cells. Immunohistochemical
352 analysis showed high *Tp53* protein expression in the parental
353 tumor and in the derived cells (Fig. 2C–D). *Tp53* expression in the
354 IGR-CaP1 cells (P16) was confirmed by Western Blot analysis with
355 the anti-*Tp53* DO-7 antibody (not shown). High *Tp53* expression
356 was assumed to correspond to the stabilized mutated *Tp53* gene
357 product. Sequencing did indeed reveal a missense mutation at the
358 nucleotide A377G corresponding to a change at codon Y126C. 359

Cell growth and kinetics 360

The IGR-CaP1 cells grew rapidly in classic culture medium
361 conditions with a doubling time of 43 h. Similar cell kinetics
362 were observed in medium containing charcoal-stripped FBS
363 (Fig. 3A). Treatment with DHT had no effect on IGR-CaP1 cell nor
364

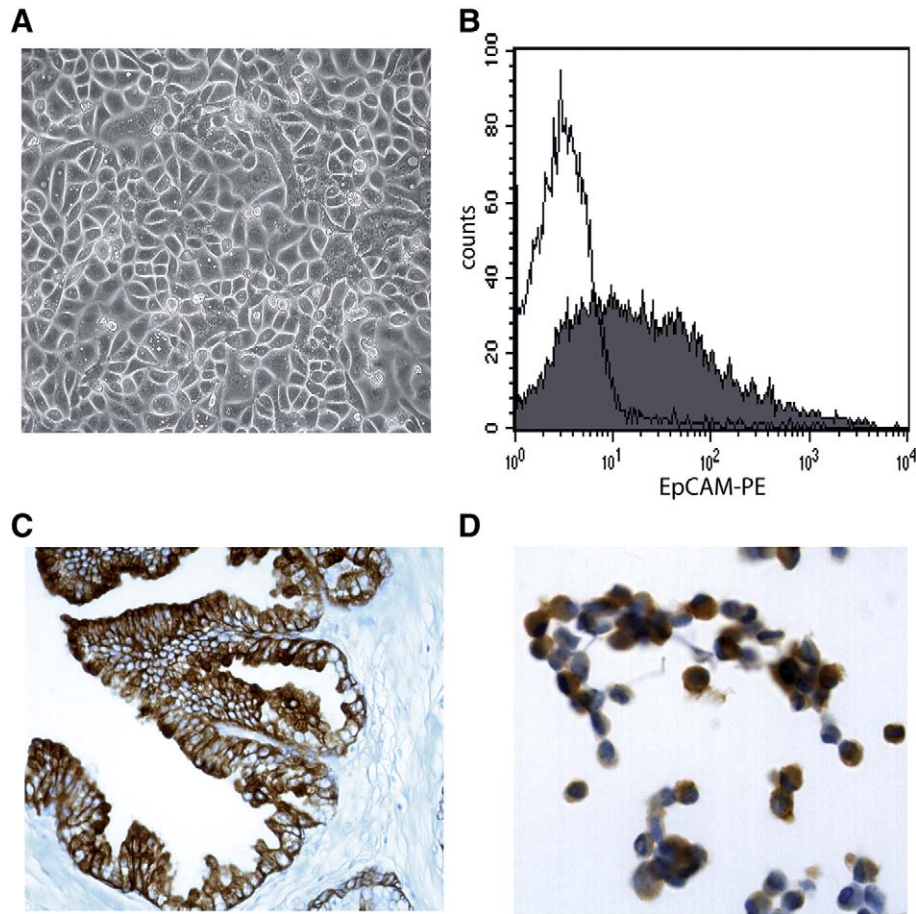


Fig. 1 – Morphology and epithelial features of the IGR-CaP1 cell line. (A) Photomicrograph of the human primary PCa cell line IGR-CaP1 (passage 29) shows typical epithelial morphology. **(B)** Expression of EpCAM was evaluated by FACS. **(C-D)** Cyokeratin expression was analyzed by IHC with anti-pan cyokeratin antibody (APK) in the initial tumor **(C)** and in IGR-CaP1 cells at passage 16 **(D)**.

Table 1 – STR analysis for identification of IGR-CaP1 cells and the two clonally-derived clones 3A11 and 3C11.

Locus ID	IGR-CaP1	3A11 clone	3C11 clone
D8S1179	13-14-15-16-17	13-14-15-16-17	13-14-15-16-17
D21S11	26-30.2	26-30.2	26-30.2
D7S820	9.1-10.1-11.2	9.1-10.1-11.2	9.1-10.1-11.2
CSF1PO	11-14-16	11-14-16	11-14-16
D3S1358	14-15	14-15	14-15
TH01	7-8-9.3	7-8-9.3	7-8-9.3
D13S317	8-10	8-10	8-10
D16S539	11-12-13	11-12-13	11-12-13
D2S1338	17-24-25	17-24-25	17-23-24
D19S433	13-14	13-14	12-13-14
vWA	16-20-21	16--19-22	16-20-21
TPOX	8-10-11	8-10-11	8-10-11
D18S51	14-15-16	15-16	15-16
Amelogenin	X	X	X
D5S818	12-13	12-13	12-13-16.1
FGA	20-21-25-26	20-21-25-26	20-21-24-26

Loci were analyzed using the multiplex-PCR-based Identifier amplification kit (Applied Biosystems), comprising 15 autosomal STR Loci and the sex-chromosome marker amelogenin.

on androgen-independent PC3 cell growth (Fig. 3B). Growth of LNCaP cells was increased through a daily treatment with 10^{-9} M DHT for 3 days to serve as a control.

IGR-CaP1 cells do not express AR or PSA but express other prostate-specific markers

IGR-CaP1 cells did not express androgen receptor protein (AR) or secretory prostate-specific antigen (PSA) as shown by blot analyses (Fig. 3C). The LNCaP and MDA-PCa-2b cells which both express these two prostate markers were used as positive controls while the PC3 cells were used as a negative control. FACS analysis confirmed the absence of PSA and AR in IGR-CaP1 cells, as compared to LNCaP and PC3 cell lines (Supplementary Fig. 1A). Furthermore, in IGR-CaP1 cells neither AR nor PSA were detected at mRNA levels by quantitative RT-PCR analyses (Fig. 3D). AR protein and PSA expression in the IGR-CaP1 cell line contrasted with that observed in the original tumor. The absence of AR and PSA expression in the early passages of the IGR-CaP1 cell line (Supplementary Fig. 1B) suggests that cells expressing AR were lost during the *in vitro* cell culture establishment. It is established that in prostatic epithelium, AR protein and PSA expression is restricted to luminal secretory prostate cells and is not observed in

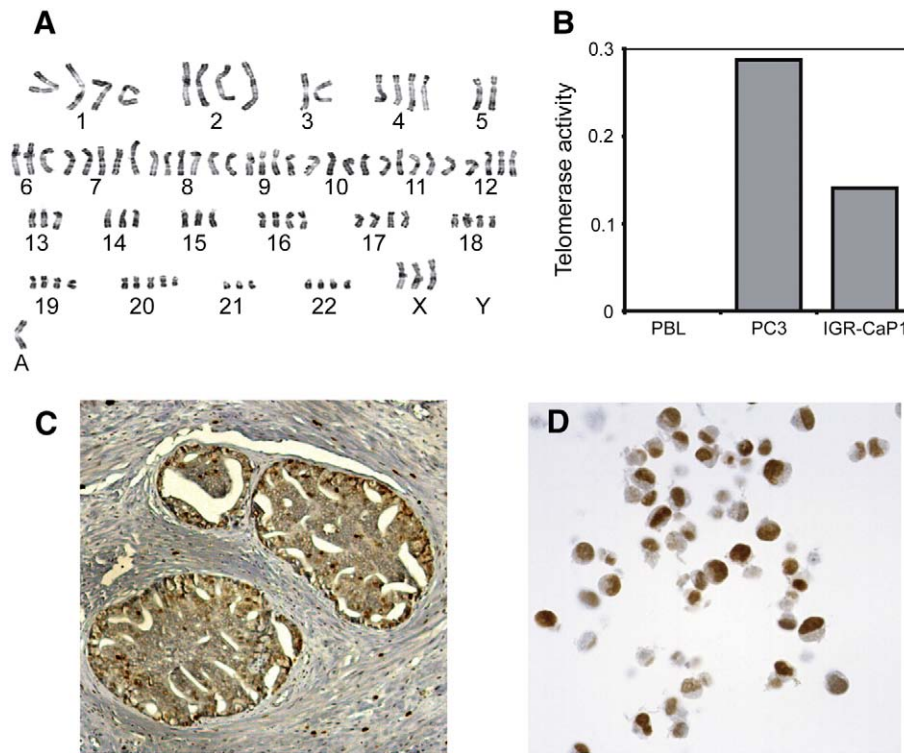


Fig. 2 – Malignancy features of the IGR-CaP1 cell line. (A) Karyotypic analysis of the IGR-CaP1 cell line using a conventional R-banding technique showing a complex tetraploid karyotype with 86-91 chromosomes. (B) Telomerase activity was quantified by quantitative PCR. Telomerase activity of IGR-CaP1 cells was compared to normal lymphocyte cells (PBL). PC3 cells were used as positive controls. (C–D) IHC showing high p53 expression in the initial prostatic tumor (C) and in the IGR-CaP1 cell line (D).

386 the basal layer cells of the epithelium, suggesting that IGR-CaP1
387 cells might correspond to basal epithelial prostate cancer cells.

388 Alpha-methylacyl-CoA-racemase (AMACR/ P504S) is a bio-
389 marker for prostate cancer that is strongly expressed in prostate
390 cancer cell lines and tissues independently of androgen receptor
391 expression [25,26]. As measured by FACS analysis, IGR-CaP1 cells
392 expressed AMACR as also observed in LNCaP cells (Fig. 3E) and in
393 PC3 cells (not shown). Like other prostate-specific markers, PSMA,
394 the prostate-specific membrane antigen (also named FOLH1) [27]
395 is expressed only in a small fraction (~2%) of IGR-CaP1 cells, as
396 shown by flow cytometer analysis, compared to LNCaP cells
397 (Fig. 3E). The low level of PSMA expression detected in *in vitro*
398 culture conditions was in accordance with PSMA expression
399 observed in orthotopic xenografts (Fig. 4B).

400 **IGR-CaP1 cells reconstitute prostate adenocarcinoma in mice**

401 To determine tumorigenicity of IGR-CaP1 cells in animals, cells were
402 injected into male nude mice both subcutaneously and orthotopi-
403 cally. Subcutaneous injections of IGR-CaP1 cells resulted in the
404 formation of palpable tumors within a week with 90% of mice (20/
405 22) bearing tumors after 6–8 weeks (Fig. 4A). Orthotopic injection of
406 IGR-CaP1 cells resulted in the formation of intraprostatic tumors
407 (Fig. 4B). In all tumors, HES staining of sections revealed glandular
408 differentiation with acini attesting the presence of adenocarcinoma.
409 Immunohistochemical staining with Ki67 revealed a high prolifer-
410 ation index which was higher in the intraprostatic tumor than in
411 subcutaneous xenografts, indicating more aggressive features in
412 orthotopic tumors (Fig. 4A and B). All the neoplastic cells expressed

413 cytokeratins, as shown with CK14 labelling (Fig. 4A), but none
414 expressed chromogranin A indicating an epithelial phenotype (not
415 shown). In addition, staining for both prostatic acid phosphatase
416 (PAP) and prostate-specific membrane antigen (PSMA) ascertained
417 the prostate origin of the tumor (Fig. 4A and B). Metastases were
418 observed in animals with both intraprostatic and subcutaneous
419 tumors and predominantly in the liver and lung (not shown).
420 Androgen responsiveness was then evaluated *in vivo* by castrating
421 animals ($n=5$), once IGR-CaP1 tumors attained a volume of
422 approximately 300 mm³. Castration resulted in a slight reduction
423 of tumor progression although the difference was not statistically
424 different (interaction p -value = 0.096) (Supplementary Fig. 2). This
425 suggests that although the androgen receptor was not expressed in
426 epithelial tumor cells, tumor progression was at least partially under
427 androgen control, thus emphasizing the importance of the tumor
428 microenvironment [28]. However, tumor progression in the castra-
429 ted mice suggested that the epithelial tumor cells might possess
430 specific properties that were contributing to the survival of tumor
431 cells in response to androgen deprivation. Altogether, these data
432 showed that tumors initiated by the IGR-CaP1 cell line recapitulate
433 the characteristics of any initial human prostate cancer in mice.

434 **IGR-CaP1 cells express high levels of basal epithelial prostate** 435 **markers**

436 To determine the phenotypes of IGR-CaP1 cells, we first examined
437 the expression of the cytokeratin markers CK5, CK8, CK14 and CK18
438 by cytometry analysis (Fig. 5A). The cytokeratin expression profile of
439 the luminal epithelial LNCaP cell line was used as a control. IGR-CaP1
439

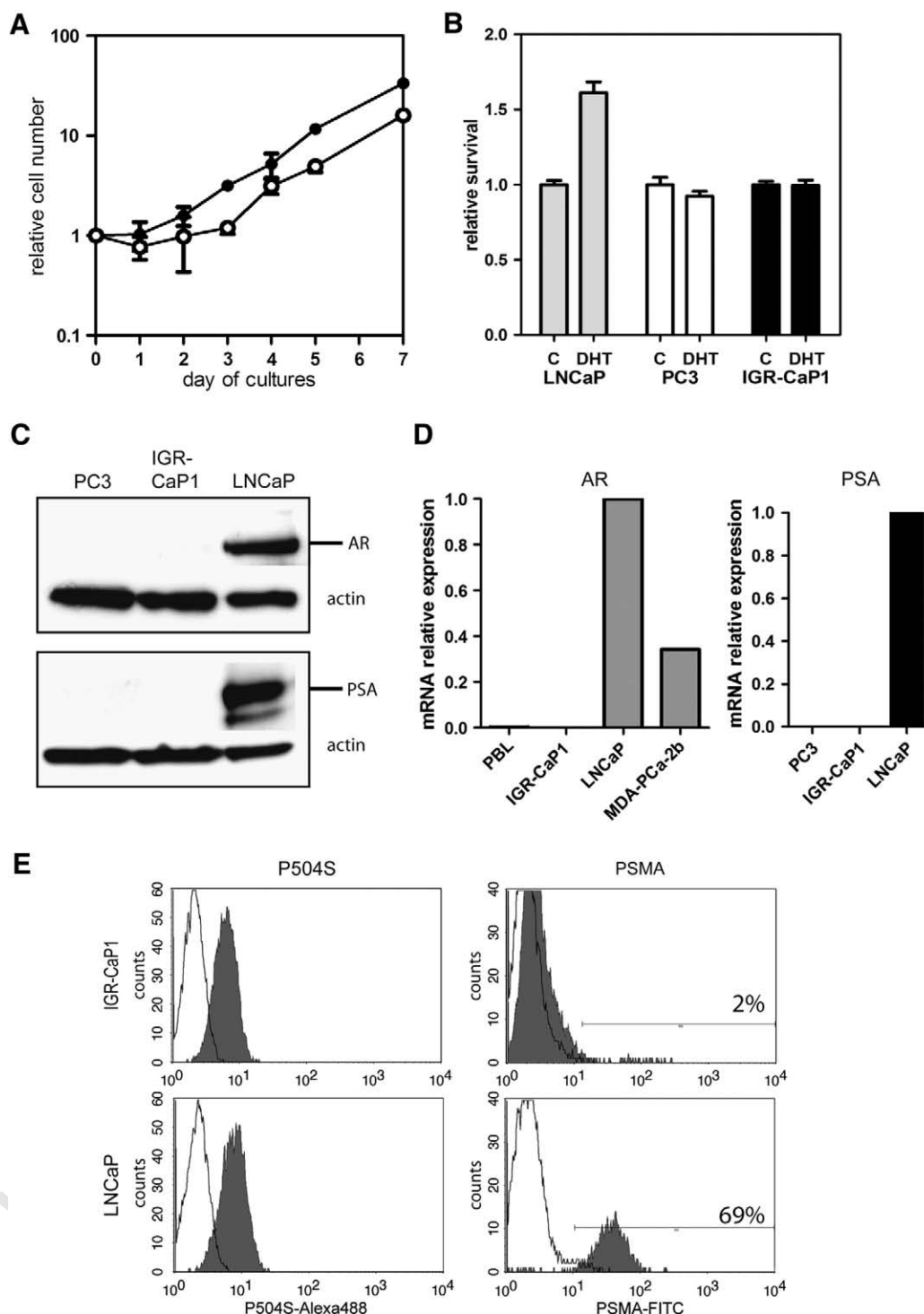


Fig. 3 – Cell growth, kinetics and expression of prostate-specific markers in IGR-CaP1 cells. (A) The growth rate of IGR-CaP1 cells at passage 28 was determined in culture medium supplemented with 10% FBS (●) or with 10% charcoal-stripped FBS (○). **(B)** The survival of IGR-CaP1, LNCaP and PC3 cells was determined after treatment of 10^{-9} M DHT for 72 h compared to no treatment (C) in medium supplemented with charcoal-stripped FBS. **(C)** Blot analysis showed no expression neither of AR nor of PSA in IGR-CaP1 cells compared to that found in PC3 and LNCaP cells respectively used as negative and positive controls. **(D)** The absence of AR and PSA gene expression was confirmed by quantitative RT-PCR analyses when compared with mRNA extracted from MDA-PCa-2b and from LNCaP cells as positive controls. **(E)** The expression level of the prostate markers P504S (AMACR) and PSMA was evaluated by flow cytometry. LNCaP cells were used as controls.

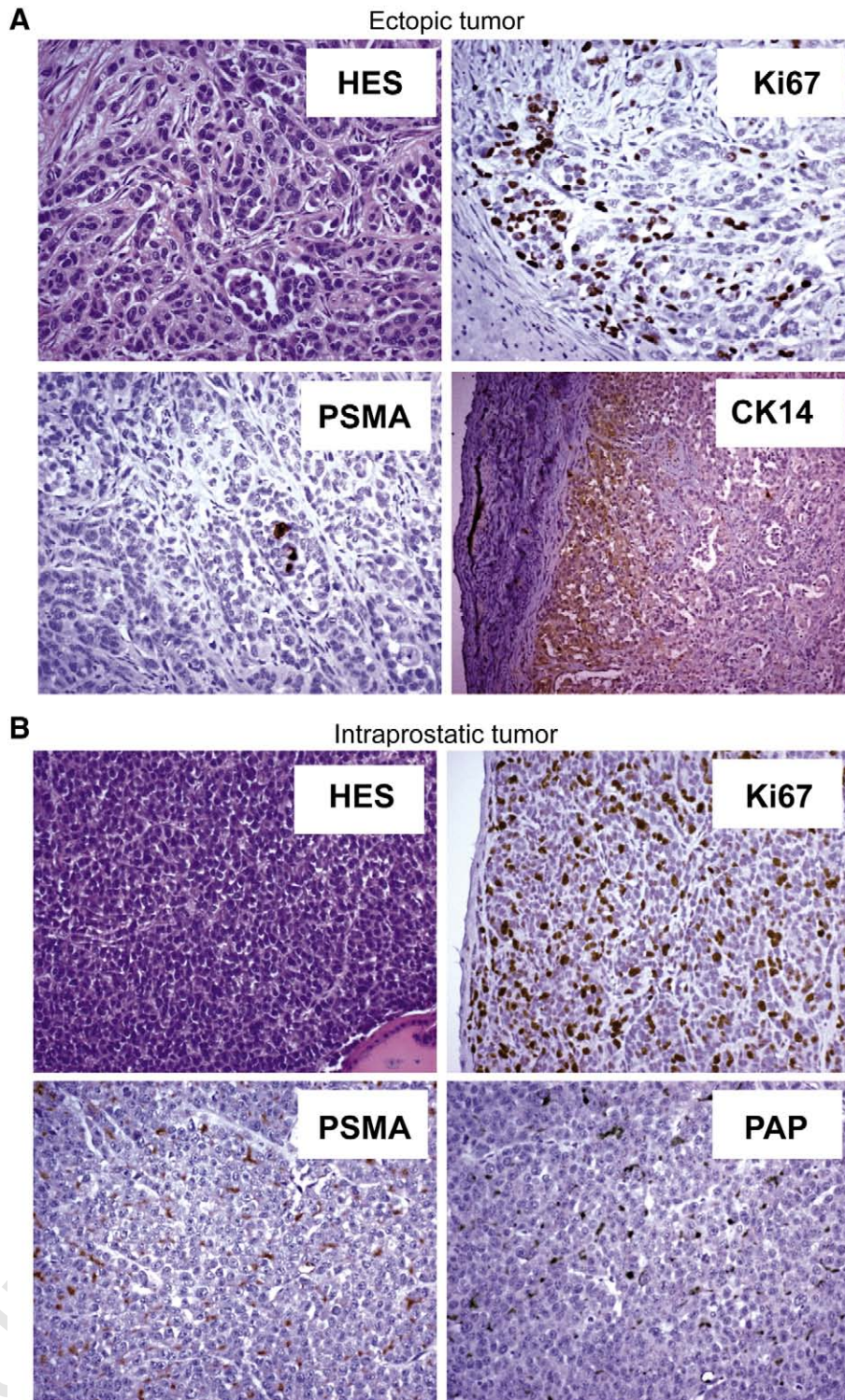


Fig. 4 – IGR-CaP1 cells reconstitute adenocarcinoma in mice. IGR-CaP1 cells were injected into male nude mice both subcutaneously (A) or intraprostatically (B). HES staining of tumor sections revealed glandular differentiation with acini confirming the presence of adenocarcinoma. CK14 attested the epithelial origin of the tumor. Ki67 staining revealed the proliferation index. Markers corresponding to prostatic acid phosphatase (PAP) and the prostate secreted membrane antigen (PSMA) confirmed the prostate origin of the tumor.

440 cells exhibited strong staining for CK5/8 and CK14 but no staining for
 441 CK8. Although adult prostate basal cells have been shown to express
 442 p63, we did not detect p63 expression in these cells (not shown). We

detected low labelling for the luminal epithelial marker CK18 in IGR- 443
 CaP1 cells compared to that observed in LNCaP cells (93% CK18 444
 fluorescence in LNCaP versus 34% in IGR-CaP1 cells). The absence of 445

446 CK8 and the low level of CK18 expression indicated the absence of
 447 luminal differentiation in cultured IGR-CaP1 cells. Additionally, CK19
 448 expression was detected in early passages of the IGR-CaP1 cell line,
 449 but disappeared during *in vitro* passaging and was not detectable in
 450 cells at passage 71 (not shown). The two clones 3A11 and 3C11
 451 exhibited roughly the same cytokeratin expression profile. These
 452 results as a whole indicate that the IGR-CaP1 cell line displays a
 453 cytokeratin profile corresponding to basal epithelial cells. As prostate
 454 stem cells have been shown to exist in the basal cell compartment,
 455 these data suggested that a small subset of these cells expressing a
 456 broad spectrum cytokeratin profile might correspond to progenitor/
 457 stem cells.

458 ***IGR-CaP1 cells and clonally-derived clones show features of*** 459 ***prostate cancer stem cells***

460 Previous studies have suggested that putative prostate progenitor/
 461 stem cells are located in the basal layer and express markers of
 462 basal cells. As in the normal prostate, the putative stem cell
 463 population was shown to be enriched in CD44 and CD133 antigens
 464 [11], we first evaluated their expression levels in the IGR-CaP1 cell
 465 line by flow cytometry (Fig. 5B). Compared to LNCaP cells in which
 466 only a minor fraction expressed CD44, almost all the IGR-CaP1 cells
 467 expressed CD44 antigen. CD133 expression was not observed in
 468 LNCaP cells. In contrast, we detected two populations in IGR-CaP1
 469 cells, one exhibiting high CD133 expression and the other was
 470 CD133-negative. CXCR4, a key molecule in the regulation of the
 471 migratory and metastatic properties of cancer cells, may be
 472 essential for the progression of the CD133⁺ prostate cancer stem
 473 cells [15]. We found that a large subset of IGR-CaP1 cells expressed
 474 the CXCR4 molecule. In addition, we found that all the IGR-CaP1
 475 cells were CD24 positive (Supplementary Fig. 3A). Real-time
 476 quantitative RT-PCR confirmed high expression of CD44 in the
 477 parental IGR-CaP1 cell line and in the clonally-derived clones 3A11
 478 and 3C11 (mean Ct of 25.8) whereas CD44 gene expression was
 479 not detectable in LNCaP cells (Ct > 40) (not shown). High
 480 expression of CD133 and CXCR4 was also confirmed by RT-PCR
 481 performed at different passages (Fig. 5C). The combined biomarker
 482 expression after triple-labelling and flow cytometry analysis was
 483 evaluated and showed a high fraction of CD44⁺/CD133⁺/CXCR4⁺
 484 triple-labelled cells (13% of the population in the parental IGR-
 485 CaP1 cells, 23% and 34% in 3A11 and 3C11 clones respectively)
 486 (Supplementary Fig. 3B). Furthermore, as it has been postulated
 487 that anchorage-independent culture of tumor cells is a useful tool
 488 for enriching and characterizing stem cells, we next investigated
 489 the clonogenic capacity in a soft agar assay. The results showed
 490 that IGR-CaP1 cells were able to form spheroids (~200 μm) in
 491 serum-supplemented RPMI medium and HES staining showed
 492 glandular-like structures with a lumen (Fig. 5D). These findings
 493 suggest that IGR-CaP1 cells possess stem cell-like characteristics.
 494 We next investigated the ability of IGR-CaP1 cells to maintain their
 495 characteristics after xenografting into animals. Cells were xeno-
 496 grafted subcutaneously into nude mice. Subsequently, after
 497 2 months of tumor growth, tumor cells were dissociated by
 498 enzymatic digestion and plated in culture dishes in classic culture
 499 conditions. After 5 passages of *in vitro* culture, stem cell markers
 500 and basal epithelial markers were assessed by FACS analysis. The
 501 results in Fig. 5E show that even after xenografting into mice and
 502 solid tumor growth, the IGR-CaP1 cells retained the characteristics
 503 of prostate basal epithelial cells (CK5 and CK14) and the potential

of CSC (CD44, CD133 and CXCR4). In particular, we still observed
 the same fraction of CD133 positive cells (~50% of the cells).
 Interestingly, CXCR4 expression was increased in these conditions
 (75% of CXCR4 positive cells). The small fraction of PSMA positive
 cells was also conserved. Thus, these results strengthened the
 value of the IGR-CaP1 model as a model system based on tumor
 stem cells originating from the basal epithelium.

IGR-CaP1 cells show a stem cell expression signature

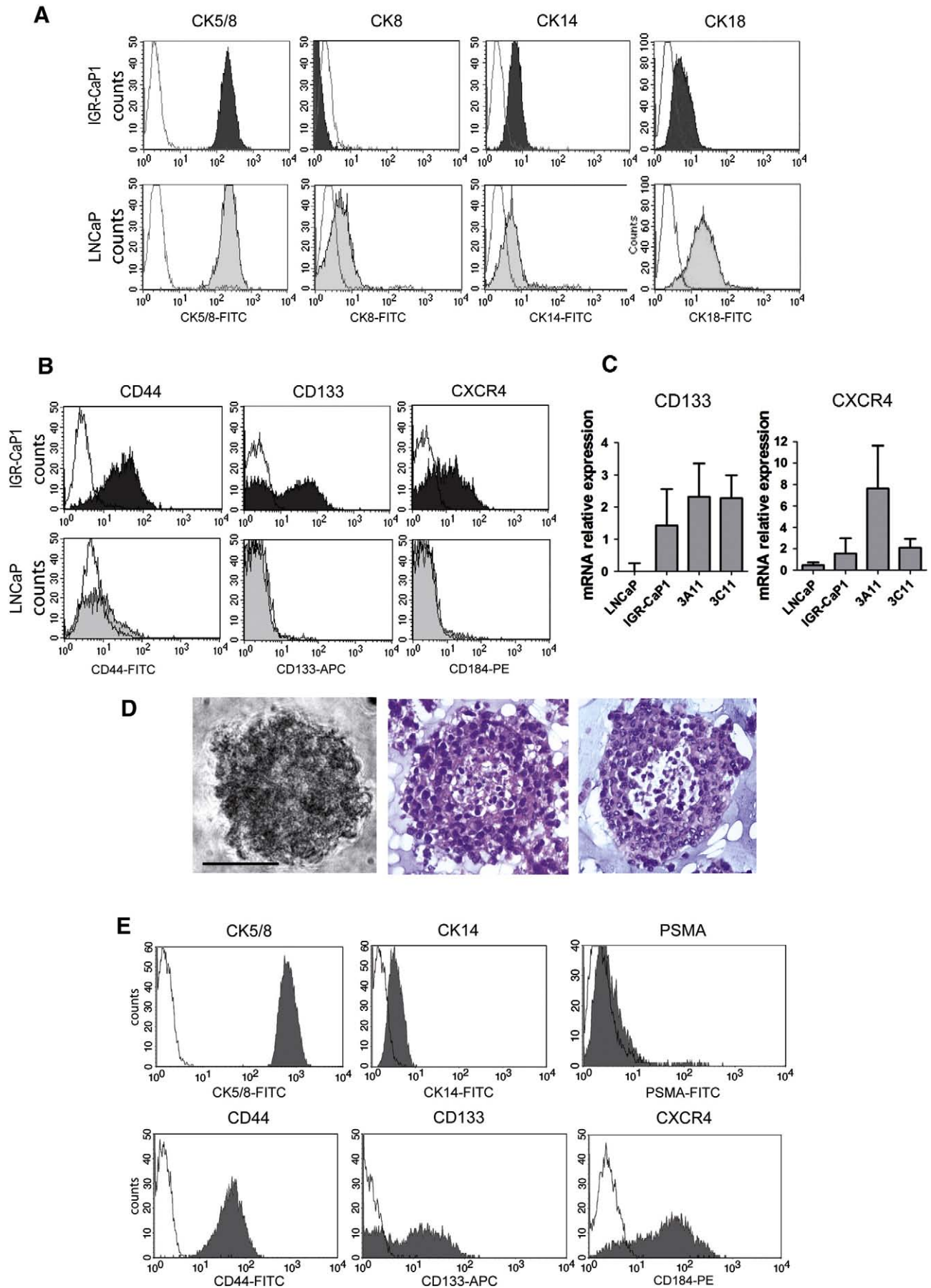
As the α2β1^{hi}/CD133⁺ phenotype is the hallmark of normal
 prostate epithelial stem cells [11], α2β1-integrin staining of IGR-
 CaP1 and clonally-derived clones was performed (Fig. 6A). High
 expression of these phenotypic markers in the IGR-CaP1 cells and
 the two clones 3A11 and 3C11, suggested the occurrence of a large
 subset of cells exhibiting the characteristics of stem cells, and
 possibly corresponding to stem cells.

We then explored whether other signalling pathways involved in
 stemness could be activated in IGR-CaP1 cells. We investigated Oct4
 which was previously reported to be expressed in pluripotent
 embryonic stem (ES) cells and in hTERT-immortalized HPE (HPET)
 cells [14,29]. Microarray analysis performed on IGR-CaP1 cells
 revealed Oct4 gene expression. By using an antibody that exclusively
 recognizes the Oct-4 (OCT4A) isoform-1, Western Blot analysis
 confirmed Oct4 expression in IGR-CaP1 cells, unlike that found in
 LNCaP and PC3 cells used as controls (Fig. 6B). Since the Hedgehog
 (HH) signalling pathway regulates key functions of stem/progenitor
 cell self-renewal [30,31], we used real-time RT-PCR to assess its
 expression in IGR-CaP1 cells compared to the LNCaP cell line. The
 SHH gene was highly expressed in IGR-CaP1 cells with concomitant
 expression of GLI1 and GLI2 target gene products. The HH receptor
 Patched protein PTCH, which normally blocks the pathway, was
 slightly downregulated in IGR-CaP1 cells (Fig. 6C). Similar results
 were obtained in the two clones 3A11 and 3C11, except for the GLI2
 gene which exhibited higher expression in the 3A11 clone and lower
 expression in the 3C11 clone.

We then assessed the expression of two other proteins which
 have been implicated in stem-like cell populations. We observed 4-
 fold higher expression of NOTCH1 gene in IGR-CaP1 cells compared to
 LNCaP cells, consistent with previous results showing that Notch gene
 expression was restricted to basal epithelial cells [32]. In agreement
 with detection of the breast cancer resistance protein BCRP/ABCG2 in
 basal epithelial CD133⁺ prostate cells [33], IGR-CaP1 cells also
 expressed a high level of mRNA coding for ABCG2 gene (Fig. 6D).
 Similar results were obtained in the two clones 3A11 and 3C11.

Discussion

Herein, we describe the establishment and characterization of a new
 prostate cancer cell line named IGR-CaP1 obtained from a primary
 prostate cancer. Although cell lines from primary prostate carcino-
 mas are among the most difficult to establish *in vitro*, we took
 advantage of the natural extracellular matrix (IGR-XC) we recently
 developed and already used successfully to obtain cell lines derived
 from human carcinomas of unknown primary [34], to obtain a new
 cell line derived from a patient with a clinically localized prostate
 cancer. The IGR-CaP1 cell line was cultured up to passage 50. Nine
 clones were derived by limiting dilution cloning and two of them,



559 3A11 and 3C11, were cultured up to passage 10. The complete
560 identification of the new IGR-CaP1 cell line was achieved using STR
561 profiling (Table 1).

562 The chromosome abnormalities confirmed malignancy in IGR-
563 CaP1 cells which exhibited a tetraploid karyotype. Given the lack of
564 prostate cancer models, telomerase-immortalized human prostate
565 epithelial (HPET) cells provide useful models since they display
566 prostate stem cell properties and also reconstitute the original
567 prostate cancer specimen [14,15,31]. We showed that IGR-CaP1 cells
568 spontaneously elicit high telomerase activity thus attesting the
569 malignant potential of these cells. Undoubtedly, the endogenously
570 hTERT-expressing IGR-CaP1 cells are more relevant to investigate
571 the early steps of prostate oncogenesis because the key regulatory
572 steps involved in telomerase activation in tumorigenesis may be
573 missed in HPET cells. Somatic *Tp53* mutations in primary tumors are
574 associated with prostate cancer progression and a propensity for
575 metastasis [35,36]. In this respect, the missense mutation identified
576 in the IGR-CaP1 cell line at position 126 of the *Tp53* correlates with
577 the high *Tp53* protein expression found in both of these *in vitro*
578 propagated cells and in the original tumor. It is possible that both
579 properties, tetraploidy and mutated *Tp53* expression, played a role
580 in the establishment of the IGR-CaP1 cell line. Indeed, reports
581 supported that tetraploid cells occur as an early step in tumor
582 formation thus, conferring a survival advantage on tumor cells
583 during the *in vitro* process [37]. Tetraploidy might have been
584 maintained due to the presence of a mutated *Tp53*. Indeed, it has
585 been shown that a “tetraploid checkpoint” is normally controlled by
586 wild-type *Tp53* to avoid the proliferation of tetraploid cells [38].

587 Interestingly, and consistent with the results obtained *in vitro*,
588 the successful engraftment of IGR-CaP1 in nude mice plus their
589 ability to metastasize to the liver and lung, enable us to propose
590 IGR-CaP1 as an invaluable experimental model of PCa. Strikingly,
591 preliminary data obtained 10 weeks after intra-tibia injections of
592 the IGR-CaP1 cells into nude mice, imaged by high-resolution
593 microCT scan, showed both osteoblastic and osteolysis lesions
594 suggesting that these cells induced bone remodelling, as regularly
595 observed in patient bone metastases (Supplementary Fig. 4).

596 IGR-CaP1 cells do not express AR nor the androgen-regulated
597 gene PSA unlike the original tumor, suggesting a selective survival
598 advantage of AR-negative cells and the loss of differentiated AR-
599 positive cells during the early steps of *in vitro* tumor culture.
600 Consistent with the lack of AR and PSA expression, the IGR-CaP1
601 cells express the basal epithelial cytokeratins, CK5 and CK14 and
602 did not express the luminal CK8 markers. This is in full agreement
603 with the working hypothesis of the occurrence of a small
604 population of epithelial stem cells in the basal cell layer, giving
605 rise to basal cells and intermediate transit-amplifying cells [31]. As
606 we also detected CK18 expression, albeit at a much lower level,

607 this strongly suggests that IGR-CaP1 cells mainly correspond to
608 basal epithelial cells and that CK18 expression may be attributed to
609 the existence of some intermediate transit-amplifying cells.

610 Considerable efforts are currently being expended to identify
611 cells at the origin of prostate cancer. A growing body of literature
612 supports that cancer lethality results from the hierarchical expansion
613 of “cancer-initiating cells” or “cancer stem cells” (CSC), which
614 function as stem-like cells to maintain malignant growth [39].
615 Several potential markers of CSCs have been used to identify putative
616 CSCs in several solid cancers and can potentially be used to isolate
617 and characterize CSCs. One of the major reported CSC markers is
618 CD133 which is a marker for both human normal prostate stem cells
619 and prostate CSC [11]. Other studies showed that putative prostatic
620 stem cells with the $\alpha2\beta1^{hi}/CD44^{+}/CD133^{+}$ phenotype were able to
621 reconstitute prostate-like acini in mice that expressed differentiated
622 cell markers [12]. More recently, co-expression of CXCR4 was
623 demonstrated in CD133⁺ human prostatic epithelial cells immor-
624 talized with hTERT [15]. We showed that IGR-CaP1 cells exhibit high
625 expression of cancer stem cell CD44, CD133 markers and CXCR4, and
626 exhibit notably a high proportion (47%) of CD133-expressing cells
627 thus clearly identifying two populations of CD133-positive and
628 CD133-negative cells. Two sub-populations were also observed
629 based on the wide difference in $\alpha2\beta1$ -integrin labelling. Therefore,
630 as multiple populations with CSC characteristics may co-exist either
631 in the same cell line or in the same tumor, this strongly suggests that
632 our cell line corresponds to CSC-derived cancer progenitor cells
633 capable of giving rise to clonal expansion. Such an assessment is fully
634 consistent with the conclusions of Campbell and Polyak, as well as
635 Adams and Strasser [40,41] suggesting that although CSCs are a
636 special subset of tumor cells, they still constitute a heterogeneous
637 population with different biological properties.

638 There are several other signalling pathways including the HH and
639 NOTCH pathways that are so far reported to be involved in the
640 maintenance of stem or progenitor cells of many adult tissues, and
641 also shown to operate in human PCa progression [42–48]. As a
642 matter of fact, Sonic Hedgehog pathway (HH-GLI) activation and
643 high expression of the NOTCH-1 gene suggest that this signalling
644 pathway could be involved in the maintenance of the “CSC-like”
645 population within the IGR-CaP1 cells. Oct-4 expression which was
646 reported in HPET cells [14,16] and seems to play a crucial role in
647 resistance to chemotherapy in lung cancer CD133+ cells [49], is also
648 detected in IGR-CaP1 cells. It is noteworthy that high expression of
649 the BCRP/ABCG2 gene provides an additional stem cell marker in the
650 IGR-CaP1 cells. Taken together, this further suggests that the self-
651 renewal genes including HH, Notch-1, Oct4 and ABCG2, may be
652 implicated in the self-renewal properties of IGR-CaP1 cells.

653 In conclusion, the IGR-CaP1 cell line is a new model of prostate
654 cancer derived from a primary tumor exhibiting high tumorigenic

Fig. 5 – Basal-type cytokeratin profile and cancer stem cell marker expression. (A) Cytokeratin marker expression was measured in IGR-CaP1 cells by FACS. LNCaP cells were used as controls. (B) The expression level of the stem cell markers CD44, CD133 and CXCR4 (also named CD184) was evaluated by flow cytometry. LNCaP cells were used as controls. (C) CD133 and CXCR4 gene expression levels were measured by QRT-PCR in IGR-CaP1 cells and in the clones 3A11 and 3C11 using a range of passages for the IGR-CaP1 cells (P26, P31, P48 and P64), P7, P8 and P10 for the 3A11 clone and P6, P7 and P9 for the 3C11 clone. Two different samples were used for the control LNCaP cell line. Results are expressed as means \pm SD and compared to the LNCaP cells as the reference. (D) Anchorage-independent growth of IGR-CaP1 cells in soft-agar assay showing spheroids grown in RPMI medium. Representative HES-stained section. Scale-bar: 100 μ m (E) Re-establishment of the IGR-CaP1 cell line after xenografting into nude mice. Basal cytokeratin profiles, stem cell markers and PSMA expression after engraftment in animals and re-establishment *in vitro* of IGR-CaP1 cells (P5). Results are representative of what was obtained in the 4 newly established cells after mouse engraftment.

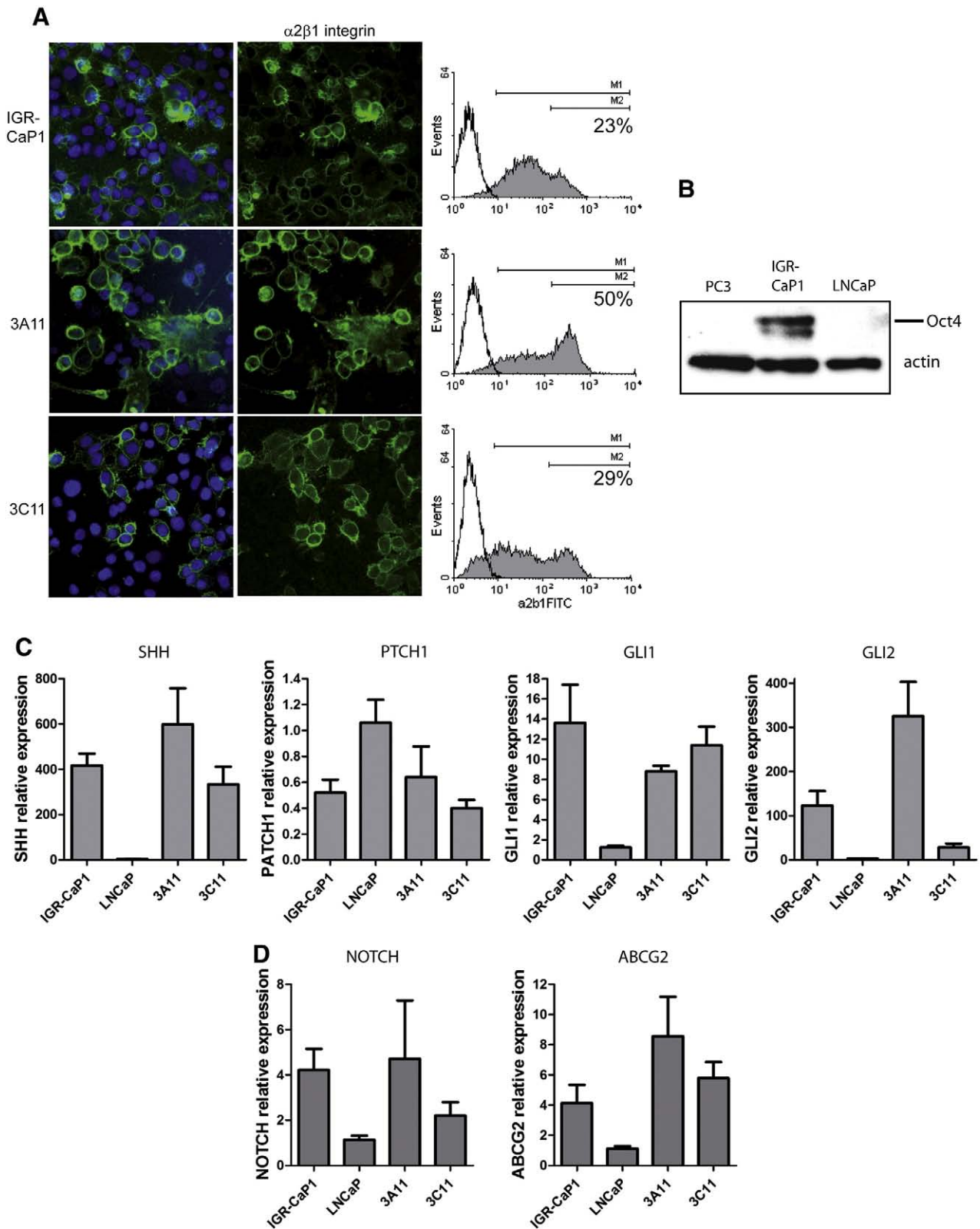


Fig. 6 – Stem cell signalling pathways in IGR-CaP1 cells. (A) $\alpha 2\beta 1$ -integrin was measured by immunofluorescence and by FACS in IGR-CaP1 cells and in the 3A11 and 3C11 clones, using anti-VLA-2 antibody. The nuclei were counterstained with Dapi. The fraction of $\alpha 2\beta 1$ integrin^{high}-expressing cells was estimated with the M2 marker (B) Oct4 expression was evaluated by blot analysis in IGR-CaP1 cell extracts and compared with that found in PC3 and LNCaP cells. (C and D) QRT-PCR was used to determine the expression level of markers identified as regulators of normal prostate stem/progenitor cells. Multiple passage levels were used as in Fig. 5C. Results are expressed as means \pm SEM and compared to the LNCaP cells used as controls.

655 properties *in vivo*. Spontaneously immortalized, these mutated
 656 Tp53 tetraploid cells express hTERT and high-level expression of
 657 stem cell markers (CD44, CD133, $\alpha 2\beta 1$ -integrin). Additionally, the
 658 IGR-CaP1 cells possess additional CSC characteristics, namely a 3D
 659 sphere-forming ability and a renewal capacity by maintaining
 660 their CSC potential after xenografting into mice. Thus, the IGR-
 661 CaP1 cell line derived from a primary tumor represents an
 662 experimental model of an aggressive prostate tumor with stem
 663 cell properties. Moreover, the stem cell signature provides an
 664 invaluable tool for investigating the mechanisms of resistance to
 665 chemotherapy and radiation. It could be used to study new
 666 therapeutic strategies both *in vitro* and *in vivo*, namely new
 667 therapeutic strategies targeting the stem cell properties of cancer
 668 cells.

669 Supplementary materials related to this article can be found
 670 online at doi:10.1016/j.yexcr.2010.10.012.
 671

673 Disclosure statement

674 This new IGR-CaP1 cell line was the subject of a European patent
 675 pending entitled “Prostate cancer cell lines and their use in
 676 screening method” deposited on the April 14th, 2009. Biological
 677 material has been deposited at the Pasteur Institut (Paris) (CNCM
 678 I-4126). The patented material will be available under a Material
 679 Transfer Agreement for research use.

680 Acknowledgments

682 We would like to thank E. Connault and F. Tabarin for excellent
 683 technical assistance. We also thank gratefully F. Commo for his
 684 help in statistical analysis. N.A.N was supported by the Association
 685 pour la Recherche sur les Tumeurs de la Prostate (ARTP) and is
 686 supported by the Association pour la Recherche sur le Cancer
 687 (ARC). D.C. is supported by ARTP (France), by the Prostate Cancer
 688 Research Foundation (PCRF, UK) and SALES Foundation (Argentina).
 689 We also thank L. Saint-Ange for editing.

690 REFERENCES

- 691 [1] A.M. Lin, E.J. Small, Prostate cancer update: 2007, *Curr. Opin.*
 692 *Oncol.* 20 (2008) 294–299.
 693 [2] K. Fizazi, N.M. Navone, Preclinical models of prostate cancer, *Bull.*
 694 *Cancer* 92 (2005) 129–141.
 695 [3] R.E. Sobel, M.D. Sadar, Cell lines used in prostate cancer research:
 696 a compendium of old and new lines-part 2, *J. Urol.* 173 (2005)
 697 360–372.
 698 [4] S. Koochekpour, G.A. Maresh, A. Katner, K. Parker-Johnson, T.J.
 699 Lee, F.E. Hebert, Y.S. Kao, J. Skinner, W. Rayford, Establishment
 700 and characterization of a primary androgen-responsive
 701 African-American prostate cancer cell line, E006AA, *Prostate* 60
 702 (2004) 141–152.
 703 [5] S.R. Selvan, A.N. Cornforth, N.P. Rao, Y.A. Reid, P.M. Schiltz, R.P.
 704 Liao, D.T. Price, F.S. Heinemann, R.O. Dillman, Establishment and
 705 characterization of a human primary prostate carcinoma cell line,
 706 HH870, *Prostate* 63 (2005) 91–103.
 707 [6] J.M. D'Antonio, D.J. Vander Griend, L. Antony, G. Ndikuyeze, S.L.
 708 Dalrymple, S. Koochekpour, J.T. Isaacs, Loss of androgen
 709 receptor-dependent growth suppression by prostate cancer cells
 710 can occur independently from acquiring oncogenic addiction to
 711 androgen receptor signalling, *PLoS ONE* 5 (2010) e11475.
 712 [7] G. Attard, S. Rizzo, I. Ledaki, J. Clark, A.H. Reid, A. Thompson,
 713 V. Khoo, J.S. de Bono, C.S. Cooper, D.L. Hudson, A novel,
 714 spontaneously immortalized, human prostate cancer cell line,
 715 Bob, offers a unique model for pre-clinical prostate cancer studies,
 716 *Prostate* 69 (2009) 1507–1520.
 717 [8] J.E. Visvader, G.J. Lindeman, Cancer stem cells in solid tumors:
 718 accumulating evidence and unresolved questions, *Nat. Rev.*
 719 *Cancer* 8 (2008) 755–768.
 720 [9] R.A. Taylor, G.P. Risbridger, The path toward identifying prostatic
 721 stem cells, *Differentiation* 76 (2008) 671–681.
 722 [10] A.T. Collins, F.K. Habib, N.J. Maitland, D.E. Neal, Identification and
 723 isolation of human prostate epithelial stem cells based on alpha
 724 (2)beta(1)-integrin expression, *J. Cell Sci.* 114 (2001) 3865–3872.
 725 [11] G.D. Richardson, C.N. Robson, S.H. Lang, D.E. Neal, N.J. Maitland, A.
 726 T. Collins, CD133, a novel marker for human prostatic epithelial
 727 stem cells, *J. Cell Sci.* 117 (2004) 3539–3545.
 728 [12] A.T. Collins, P.A. Berry, C. Hyde, M.J. Stower, N.J. Maitland,
 729 Prospective identification of tumorigenic prostate cancer stem
 730 cells, *Cancer Res.* 65 (2005) 10946–10951.
 731 [13] B. Daly-Burns, T.N. Alam, A. Mackay, J. Clark, C.J. Shepherd,
 732 S. Rizzo, R. Tatoud, M.J. O'Hare, J.R. Masters, D.L. Hudson, A
 733 conditionally immortalized cell line model for the study of human
 734 prostatic epithelial cell differentiation, *Differentiation* 75 (2007)
 735 35–48.
 736 [14] G. Gu, J. Yuan, M. Wills, S. Kasper, Prostate cancer cells with stem
 737 cell characteristics reconstitute the original human tumor *in vivo*,
 738 *Cancer Res.* 67 (2007) 4807–4815.
 739 [15] J. Miki, B. Furusato, H. Li, Y. Gu, H. Takahashi, S. Egawa, I.A. Sesterhenn,
 740 D.G. McLeod, S. Srivastava, J.S. Rhim, Identification of putative stem
 741 cell markers, CD133 and CXCR4, in hTERT-immortalized primary
 742 nonmalignant and malignant tumor-derived human prostate
 743 epithelial cell lines and in prostate cancer specimens, *Cancer Res.* 67
 744 (2007) 3153–3161.
 745 [16] H. Li, J. Zhou, J. Miki, B. Furusato, Y. Gu, S. Srivastava, D.G. McLeod,
 746 J.C. Vogel, J.S. Rhim, Telomerase immortalized non-malignant
 747 human prostate epithelial cells retain the properties of
 748 multipotent stem cells, *Exp. Cell Res.* 314 (2008) 92–102.
 749 [17] E. Ferrandis, J. Da Silva, G. Riou, J. Bénard, Coactivation of the
 750 MDR1 and MYCN genes in human neuroblastoma cells during the
 751 metastatic process in the nude mouse, *Cancer Res.* 54 (1994)
 752 2256–2261.
 753 [18] W.W. Kao, D.J. Prockop, Proline analogue removes fibroblasts
 754 from cultured mixed cell populations, *Nature* 266 (1977) 63–66.
 755 [19] K. Fizazi, J. Yang, S. Peleg, C.R. Sikes, E.L. Kreimann, D. Daliani,
 756 M. Olive, K.A. Raymond, T.J. Janus, C.J. Logothetis, G. Karsenty, N.
 757 M. Navone, Prostate cancer cells-osteoblast interaction shifts
 758 expression of growth/survival-related genes in prostate cancer
 759 and reduces expression of osteoprotegerin in osteoblasts, *Clin.*
 760 *Cancer Res.* 9 (2003) 2587–2597.
 761 [20] Z.P. Pavelic, H.K. Slocum, Y.M. Rustum, P.J. Creaven, N.J. Nowak,
 762 C. Karakousis, H. Takita, A. Mittelman, Growth of cell colonies in
 763 soft agar from biopsies of different human solid tumors, *Cancer*
 764 *Res.* 40 (1980) 4151–4158.
 765 [21] M. Eura, K. Chikamatsu, F. Katsura, A. Obata, Y. Sobao, M. Takiguchi,
 766 Y. Song, E. Appella, T.L. Whiteside, A.B. DeLeo, A wild-type sequence
 767 p53 peptide presented by HLA-A24 induces cytotoxic T
 768 lymphocytes that recognize squamous cell carcinomas of the head
 769 and neck, *Clin. Cancer Res.* 6 (2000) 979–986.
 770 [22] J. Couturier, B. Dutrillaux, Conservation of replication chronology
 771 of homologous chromosome bands between four species of the
 772 genus *Cebus* and man, *Cytogenet. Cell Genet.* 29 (1981) 233–240.
 773 [23] K. Fizazi, C.R. Sikes, J. Kim, J. Yang, L.A. Martinez, M.C. Olive, C.J.
 774 Logothetis, N.M. Navone, High efficacy of docetaxel with and
 775 without androgen deprivation and estramustine in preclinical
 776 models of advanced prostate cancer, *Anticancer Res.* 24 (2004)
 777 2897–2903.
 778

- 779 [24] C.M. Counter, W.C. Hahn, W. Wei, S.D. Caddle, R.L. Beijersbergen, 823
 780 P.M. Lansdorp, J.M. Sedivy, R.A. Weinberg, Dissociation among in 824
 781 vitro telomerase activity, telomere maintenance, and cellular 825
 782 immortalization, *Proc. Natl Acad. Sci. USA* 95 (1998) 826
 783 14723–14728. 827
- Q1 784 [25] Z. Jiang, B.A. Woda, K.L. Rock, Y. Xu Test, *Am. J. Surg. Pathol.* 25 828
 785 (2001) 1397–1404. 829
- 786 [26] S. Zha, S. Ferdinandusse, S. Denis, R.J. Wanders, C.M. Ewing, J. Luo, 830
 787 A.M. De Marzo, W.B. Isaacs, Alpha-methylacyl-CoA racemase as 831
 788 an androgen-independent growth modifier in prostate cancer, 832
 789 *Cancer Res.* 63 (2003) 7365–7376. 833
- 790 [27] M.J. Burger, M.A. Tebay, P.A. Keith, H.M. Samaratunga, J. Clements, 834
 791 M.F. Lavin, R.A. Gardiner, Expression analysis of delta-catenin and 835
 792 prostate-specific membrane antigen: their potential as diagnostic 836
 793 markers for prostate cancer, *Int. J. Cancer* 100 (2002) 228–237. 837
- 794 [28] L.W. Chung, A. Baseman, V. Assikis, H.E. Zhau HE, Molecular 838
 795 insights into prostate cancer progression: the missing link of 839
 796 tumor Microenvironment, *J. Urol.* 173 (2005) 10–20. 840
- 797 [29] M. Boiani, H.R. Scholer, Regulatory networks in embryo-derived 841
 798 pluripotent stem cells, *Nat. Rev. Mol. Cell Biol.* 6 (2005) 872–884. 842
- 799 [30] P.A. Beachy, S.S. Karhadkar, D.M. Berman, Tissue repair and stem 843
 800 cell renewal in carcinogenesis, *Nature* 432 (2004) 324–331. 844
- 801 [31] I.V. Litvinov, D.J. Vander Griend, Y. Xu, L. Antony, S.L. Dalrymple, J. 845
 802 T. Isaacs, Low-calcium serum-free defined medium selects for 846
 803 growth of normal prostatic epithelial stem cells, *Cancer Res.* 66 847
 804 (2006) 8598–8607. 848
- 805 [32] J. Shou, S. Ross, H. Koepfen, F.J. de Sauvage, W.Q. Gao, Dynamics 849
 806 of notch expression during murine prostate development and 850
 807 tumorigenesis, *Cancer Res.* 61 (2001) 7291–7297. 851
- 808 [33] L.E. Pascal, A.J. Oudes, T.W. Petersen, Y.A. Goo, L.S. Walashek, L.D. 852
 809 True, A.Y. Liu, Molecular and cellular characterization of ABCG2 in 853
 810 the prostate, *BMC Urol.* 6 (2007) 6. 854
- 811 [34] D. Lequin, K. Fizazi, S. Toujani, S. Souquère, M.C. Mathieu, 855
 812 P. Hainaut, A. Bernheim, F. Praz, P. Busson, Biological 856
 813 characterization of two xenografts derived from human CUPs 857
 814 (carcinomas of unknown primary), *BMC Cancer* 7 (2007) 225. 858
- 815 [35] N.M. Navone, P. Troncoso, L.L. Pisters, T.L. Goodrow, J.L. Palmer, 859
 816 W.W. Nichols, A.C. von Eschenbach, C.J. Conti, p53 protein 860
 817 accumulation and gene mutation in the progression of human 861
 818 prostate carcinoma, *J. Natl Cancer Inst.* 85 (1993) 1657–1669. 862
- 819 [36] N.M. Navone, M.E. Labate, P. Troncoso, L.L. Pisters, C.J. Conti, A.C. von 863
 820 Eschenbach, C.J. Logothetis, p53 mutations in prostate cancer bone 864
 821 metastases suggest that selected p53 mutants in the primary site 865
 822 define foci with metastatic potential, *J. Urol.* 161 (1999) 304–308. 866
 867
- [37] Z. Storchova, C. Kuffer, The consequences of tetraploidy and 823
 aneuploidy, *J. Cell Sci.* 121 (2008) 3859–3866. 824
- [38] P.R. Andreassen, O.D. Lohez, F.B. Lacroix, R.L. Margolis, Tetraploid 825
 state induces p53-dependent arrest of nontransformed 826
 mammalian cells in G1, *Mol. Biol. Cell* 12 (2001) 1315–1328. 827
- [39] M.S. Wicha, S. Liu, G. Dontu, Cancer stem cells: an old idea—a 828
 paradigm shift, *Cancer Res.* 66 (2006) 1883–1890. 829
- [40] L.L. Campbell, K. Polyak, Breast tumor heterogeneity: Cancer stem 830
 cells or clonal evolution? *Cell Cycle* 6 (2007) 2332–2338. 831
- [41] J.M. Adams, A. Strasser, Is tumor growth sustained by rare cancer 832
 stem cells or dominant clones? *Cancer Res.* 68 (2008) 4018–4021. 833
- [42] P. Sanchez, A.M. Hernández, B. Stecca, A.J. Kahler, A.M. DeGueme, 834
 A. Barrett, M. Beyna, M.W. Datta, S. Datta, A. Ruiz, i Altaba, 835
 Inhibition of prostate cancer proliferation by interference with 836
 Sonic Hedgehog-GLI1 signaling, *Proc. Natl Acad. Sci. USA* 101 837
 (2004) 12561–12566. 838
- [43] S.S. Karhadkar, G.S. Bova, N. Abdallah, S. Dhara, D. Gardner, 839
 A. Maitra, J.T. Isaacs, D.M. Berman, P.A. Beachy, Hedgehog 840
 signalling in prostate regeneration, neoplasia and metastasis, 841
Nature 431 (2004) 707–712. 842
- [44] T. Sheng, C. Li, X. Zhang, S. Chi, N. He, K. Chen, F. McCormick, 843
 Z. Gatalica, J. Xie, Activation of the hedgehog pathway in 844
 advanced prostate cancer, *Mol. Cancer* 3 (2004) 29. 845
- [45] B.Y. Chen, J.Y. Liu, H.H. Chang, C.P. Chang, W.Y. Lo, W.H. Kuo, C.R. 846
 Yang, D.P. Lin, Hedgehog is involved in prostate basal cell 847
 hyperplasia formation and its progressing towards 848
 tumorigenesis, *Biochem. Biophys. Res. Commun.* 357 (2007) 849
 1084–1089. 850
- [46] S. Thiyagarajan, N. Bhatia, S. Reagan-Shaw, D. Cozma, A. 851
 Thomas-Tikhonenko, N. Ahmad, V.S. Spiegelman, Role of GLI2 852
 transcription factor in growth and tumorigenicity of prostate 853
 cells, *Cancer Res.* 67 (2007) 10642–10646. 854
- [47] M. Zayzafoon, S.A. Abdulkadir, J.M. McDonald, Notch signaling 855
 and ERK activation are important for the osteomimetic properties 856
 of prostate cancer bone metastatic cell lines, *J. Biol. Chem.* 279 857
 (2004) 3662–3670. 858
- [48] N. Scorey, S.P. Fraser, P. Patel, C. Pridgeon, M.J. Dallman, M.B. 859
 Djamgoz, Notch signalling and voltage-gated Na1 channel activity 860
 in human prostate cancer cells: independent modulation of in 861
 vitro motility, *Prostate Cancer Prostatic Dis.* 9 (2006) 399–406. 862
- [49] Y.C. Chen, H.S. Hsu, Y.W. Chen, T.H. Tsai, C.K. How, C.Y. Wang, S.C. 863
 Hung, Y.L. Chang, M.L. Tsai, Y.Y. Lee, H.H. Ku, S.H. Chiou, Oct-4 864
 expression maintained cancer stem-like properties in lung 865
 cancer-derived CD133-positive cells, *PLoS ONE* 3 (2008) e2637. 866